

# Development of a Hodoscope for Testing and Characterization of WCD configurations for SWGO

**Luís Miguel Domingues Mendes,<sup>a,b,\*</sup> Ulisses Barres de Almeida,<sup>a</sup> Guilherme Ferreira Franco<sup>a</sup> and Luiz Augusto Stuani Pereira,<sup>c</sup> for the SWGO Collaboration**

<sup>a</sup>*Centro Brasileiro de Pesquisas Físicas - CBPF,  
Rio de Janeiro, RJ, Brazil*

<sup>b</sup>*Centro Federal de Educação Tecnológica Celso Suckow da Fonseca - CEFET-RJ,  
Rio de Janeiro, RJ, Brazil*

<sup>c</sup>*Instituto de Física, Universidade de São Paulo - IFUSP,  
São Paulo, SP, Brazil*

E-mail: [mendes@cbpf.br](mailto:mendes@cbpf.br)

We describe a hodoscope system designed for the testing and characterization of Water Cherenkov Detectors (WCDs) for the Southern Wide-field Gamma-ray Observatory (SWGO). The SWGO is an international collaboration aiming to build the first wide-field gamma-ray observatory in the southern hemisphere, using a ground array of WCDs for detecting and reconstructing Extensive Air Showers (EAS) initiated by gamma-rays with energies from a few hundred GeV to the PeV range. The hodoscope was developed at the Brazilian Center for Physics Research (CBPF) in Rio de Janeiro to support the design, calibration, and validation of different WCD configurations. The setup combines four MARTA-type RPC detectors operating in avalanche mode with a top plane of plastic scintillators, enabling precise muon tracking and coincidence triggering. The structure was designed to support different tank sizes. The system uses MAROC3 front-end ASICs and Altera Cyclone IV FPGAs for readout, all synchronized via a central control unit based on an Altera Cyclone V FPGA with an embedded Linux operating system. A comprehensive Geant4-based simulation framework was also developed to model the detector response to secondary cosmic rays. In this contribution, we present the design, current status, and early characterization results of the hodoscope, highlighting its role as a key R&D facility for SWGO.

39th International Cosmic Ray Conference (ICRC2025)  
15–24 July 2025  
Geneva, Switzerland



**ICRC 2025**  
The Astroparticle Physics Conference  
Geneva July 15-24, 2025

\*Speaker

## 1. Introduction

The Southern Wide-Field Gamma-Ray Observatory (SWGO) is a ground-based facility under development [1], to be installed in the Atacama Astronomical Park, in Chile.

The main goal is to measure the flux of gamma-rays from hundreds of GeV to the PeV scale. This will be done through the detection, identification, and reconstruction of Extensive Air Showers (EAS) initiated by gamma-rays, measuring the EAS secondary particles at ground level in a high-altitude location (4770 m).

The observatory will employ an array of Water Cherenkov Detectors (WCDs): tanks filled with purified water, and coated with UV-reflective internal walls. The tanks are instrumented with photomultiplier tubes (PMTs) to detect the Cherenkov radiation emitted by relativistic charged EAS particles as they cross the water volume.

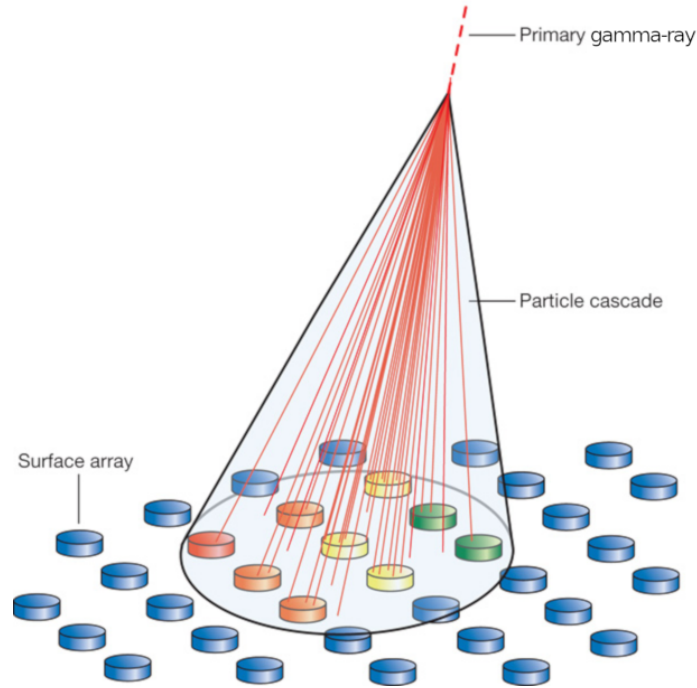


**Figure 1:** Schematic diagram of the detection of EAS particles by a surface array at ground level. Retrieved from [2].

A laboratory test facility is important to complement the numerous software simulations that have been performed to assess detector performance. A critical requirement for the facility is the flexibility in accommodating different experimental setups, allowing us to test the response of multiple detector configurations - with their respective electronics - to incoming EAS particles, and in particular atmospheric muons.

For this purpose, a hodoscope set-up was developed in CBPF, Rio de Janeiro, combining resistive plate chambers (RPC) and plastic scintillator detectors, in order to register the trajectory of crossing muons, trigger the WCD electronics in coincidence, and correlate the data between the hodoscope and the WCD for calibration. The resulting data can be used for different analyses, such

as establishing the Vertical Equivalent Muon (VEM) of the detector and analyzing the direction-dependent response in multiple PMT configurations.

## 2. Overall structure and detectors

The CBPF hodoscope has two primary parts: the bottom layer, consisting of 4 RPCs, and the top layer, formed by a plastic scintillator detector. The WCD is placed in the middle, as shown in Figure 2.

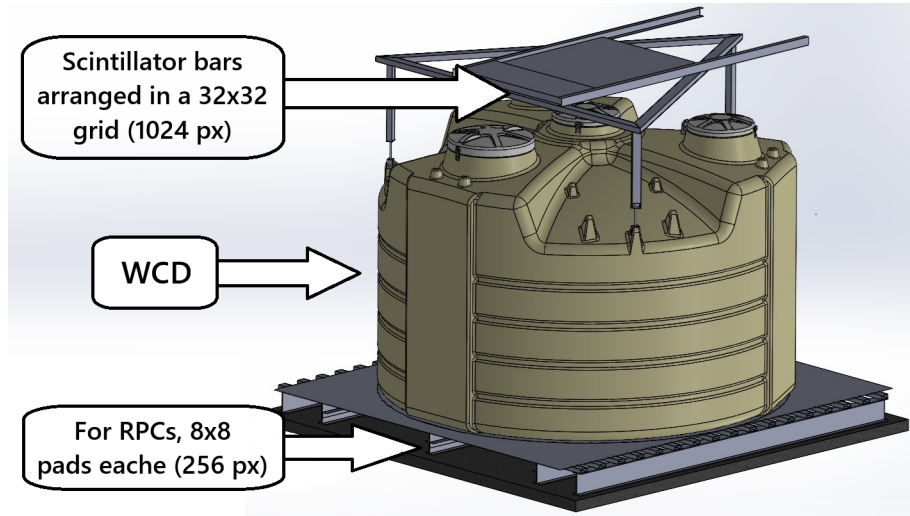


**Figure 2:** General layout of the hodoscope.

The bottom RPC detector is encased in a steel structure below the tank, capable of withstanding 40 metric tons of weight above it. The RPCs come from the MARTA project [3], they operate in avalanche mode and have their detection plane subdivided into 64 pads, of 19x15 cm effective area each. Together, they total a sensitive area of 7.3 m<sup>2</sup> with 256 pads.

The top detector, on the other hand, sits above a lightweight aluminum structure mounted on the tank's lifting lugs, with enough room for sliding along the horizontal axis. The detector is made of 64 scintillator bars, each measuring 160 × 5 × 2 cm, employing a wavelength-shifting fiber cable through its center, plus a silicon photomultiplier (SiPM) for signal collection and transduction. They're arranged in a grid of 32 lines and 32 columns, forming 1024 pixels of 5x5 cm, totaling a sensitive area of 2.56 m<sup>2</sup>.

The structure was made in such a way that the tank installed in the middle can be swapped to test different WCD configurations. At CBPF, two HDPE tanks are currently available, one with 1.7 m water height and 3.6 m diameter, and the other being able to accommodate up to 3.0 m in water height, with a footprint of 3.0 m in diameter. Both WCD units currently available at CBPF have a carbon-black inner surface layer, thus allowing testing of tank configurations with an absorbing (bare) or reflective (Tyvek-lined) interior. Both tanks can also accommodate different PMT arrangements. The structure is currently mounted with the shallow tank configuration, as shown in figure 6.

Currently, the setup has been mounted with the 1.7 m water column tank, which was originally made for the "Mercedes" Shallow Tank proposal [4]).

### 3. Hardware and Capabilities

Both the RPC and the scintillator detectors use the same model of Front-End hardware, a board with a MAROC 3 [5] (Multi-Anode ReadOut Chip) and a Cyclone IV FPGA [6]. These chips allow the Front-End to amplify and discriminate 64 channels independently, sampling them at a rate of 80 MHz, storing the discriminated data in a 128-sample deep, 64-bit wide FIFO. The programmable amplifiers in the MAROC 3 chip allow it to work both with SiPMs and RPC pads.

The Front-Ends are connected through CAT6 UTP cables to a Central Unit, a DE10-Standard [7] board equipped with a custom interface board to allow interface with UTP cables with RJ45 connectors. The board has a System-on-Chip (SoC) integrating a Cyclone V FPGA and an ARM Cortex-A9 processor, which allow exploring the advantages of both an FPGA and an ordinary CPU.

The firmware in the Central Unit's FPGA handles all functionalities that require parallelism, precise timing and fast response, such as the communication protocol with the Front-Ends and the trigger systems. It also runs an embedded OS (Angstrom Linux), allowing regular software to interface directly with the firmware, handling the higher level tasks of the acquisition system, such as remote control and access through the internet, as well as the slow control systems for the detectors (temperature and voltage monitoring, etc). Figure 3 shows an scheme of the Front-End electronics.

Even with the bottleneck of storage speed in the Central Unit memory card, the system can easily handle over 2 kHz of events, which exceeds the total coincident flux through the setup (around 200 muons/s) by an order of magnitude .

The Central Unit will send coincidence triggers with identifiers to the electronics of the WCD unit under test, to make the correlation between hodoscope and WCD events possible.

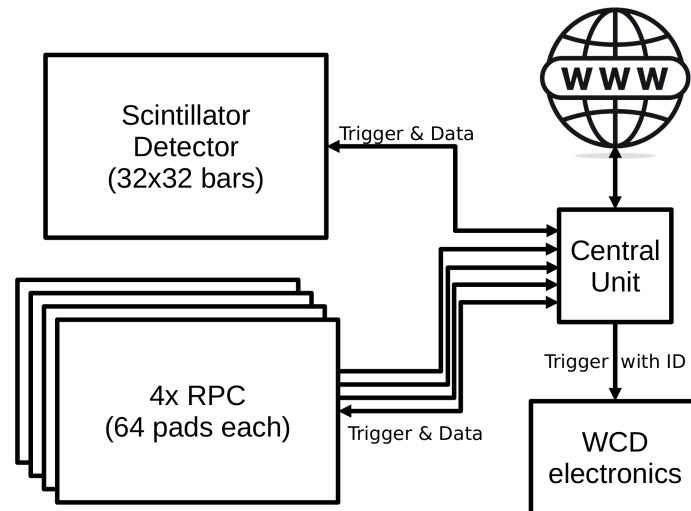


**Figure 3:** Simplified block diagram of the setup. Each detector has its own front-end electronics, and all of them connect to the Central Unit, which manages the trigger. The WCD electronics may have direct connection with the internet, but events can be stored with the received identifiers for correlation *a posteriori*.

#### 4. Simulation of the Hodoscope Setup

To study the response of the hodoscope to secondary muons and electrons from extensive air showers (EAS), a two-stage simulation framework was developed.

In the first stage, ground-level secondary particles were generated using the Cosmic-Ray Shower Library (CRY), a software toolkit that generates realistic secondary particle fluxes from cosmic-ray-induced EAS at various altitudes, including at sea level [8], accounting for geomagnetic cutoff and solar cycle effects.

For this study, secondary particle fluxes at sea level were generated for the geographic coordinates of Rio de Janeiro, Brazil ( $-22.9^\circ$  S), with geomagnetic and solar modulation settings corresponding to a specific date to reflect the 11-year solar cycle [9].

In the second stage, these particles were propagated through the WCD and detected on a simulated PMT within the WCD, using the Geant4 Monte Carlo simulation toolkit. This approach enables a detailed characterization of the energy deposition, Cherenkov photon production, and resulting signals at the PMT.

##### 4.1 Geant4-Based Detector Simulation Framework

The geometry of the hodoscope was implemented using the Geant4 simulation toolkit. Geant4 (GEometry ANd Tracking)<sup>1</sup> is a widely used framework for simulating the interactions of electromagnetic and hadronic radiation with matter [10]. Electromagnetic processes, including Cherenkov photon production and propagation, were modeled using the G4EmStandardPhysics package, the recommended physics constructor for high-energy applications [11]. Figure 4 presents the top view (left) and the bottom view (right) of the Geant4 simulation of the hodoscope geometry.

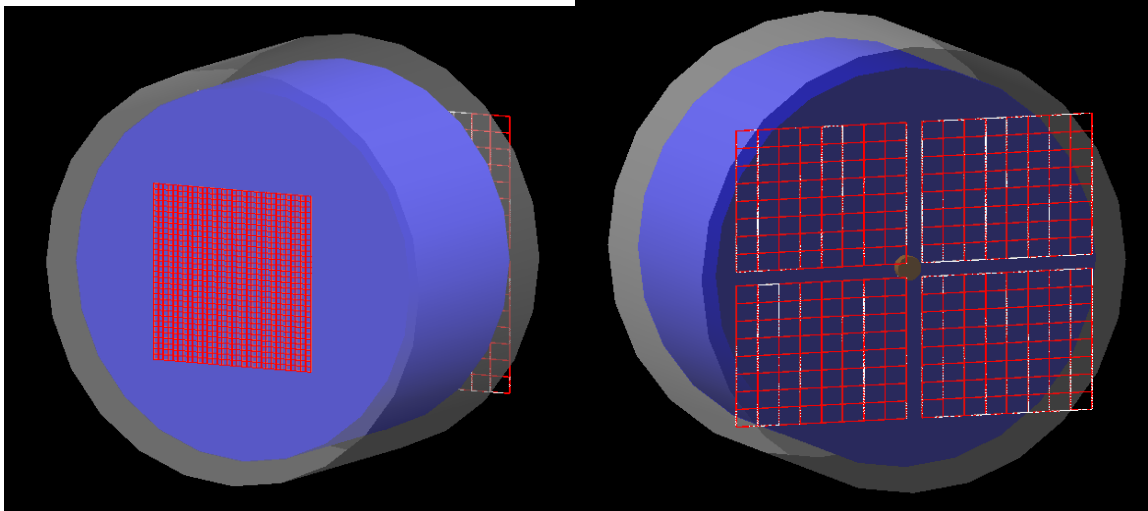


**Figure 4:** Top view (left) and bottom view (right) of the Geant4 simulation of the hodoscope geometry. The WCD has dimensions of  $3.6 \text{ m} \times 3.6 \text{ m} \times 2.1 \text{ m}$ . A scintillator panel with dimensions  $160 \text{ cm} \times 160 \text{ cm}$  is placed on top of the WCD, while four RPCs, each measuring  $152 \text{ cm} \times 120 \text{ cm}$ , are positioned at the bottom. The PMT is also located at the bottom (interior) of the tank.

<sup>1</sup><https://geant4.web.cern.ch/>

Before simulating the full hodoscope, and in order to compare the simulation with a known reference, the first runs were made to characterise the standalone WCD response to the flux of secondary EAS particles generated in the first step (as in a self-trigger setup).

This simulation thus focuses on the charge spectra (histograms of integrated ADC counts) induced in the WCD's PMT, from the interaction of the secondary muons and electrons from the EAS with the detector water volume.

These particles interact with water primarily through ionization processes. Due to their higher mass and lower interaction cross-section, muons deposit energy in a relatively uniform and linear manner along their trajectories, with an average energy deposition of approximately 0.39 GeV. Electrons, on the other hand, experience substantial multiple scattering and initiate electromagnetic cascades, resulting in more localized and variable energy losses, with an average deposited energy of approximately 0.04 GeV. These interactions lead to the emission of Cherenkov radiation, with muons producing on average  $1.2 \times 10^5$  Cherenkov photons per event, compared to approximately  $6.7 \times 10^2$  photons generated by electrons. Furthermore, muons may undergo decay within the detector medium, yielding secondary electrons that also contribute to the overall Cherenkov photon yield.

Assuming a photocathode quantum efficiency of 25% and a PMT gain of  $10^7$ , the total charge spectrum reflects the combined contributions from crossing muons, muon decays, and secondary electrons produced within the detector volume, and exhibits a prominent peak at approximately 96.7 pC. Isolating the contribution from crossing muons, which traverse the detector along relatively straight paths, the charge spectrum peaks at 82.2 pC. For muons that decay inside the WCD, the spectrum peaks at 30.7 pC, corresponding to the Cherenkov light produced by decay electrons. Secondary electrons generated through muon interactions with the detector medium produce a lower charge peak at 16.6 pC. Additionally, incident cosmic-ray electrons yield a charge spectrum peaking at 29.5 pC. The overall spectral shape and peak structure are consistent with previous observations reported by the Pierre Auger Collaboration in their study of muon decays in water-Cherenkov detectors [12].

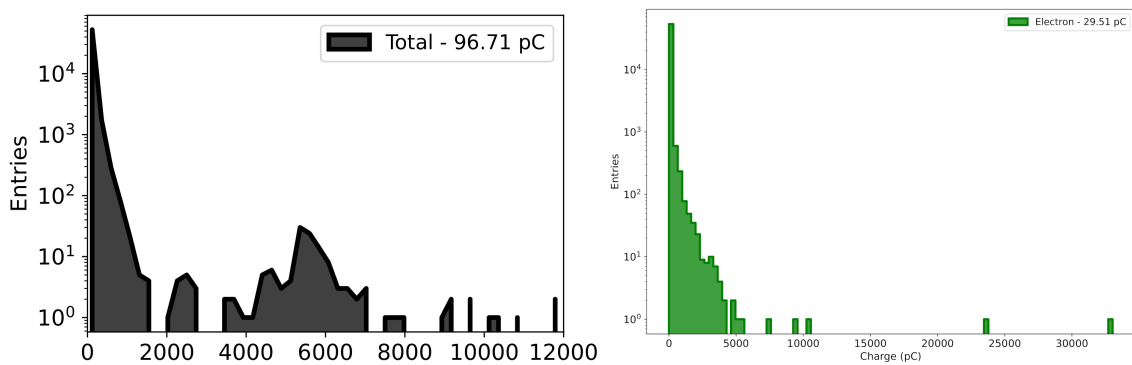


**Figure 5:** Charge spectrum measured by the PMT for cosmic-ray muons (left) and electrons (right) interacting with the WCD. The muon charge spectrum peaks at approximately 82.2 pC, being the result of different processes (crossing muons, decaying muons and secondary electrons). The electron charge spectrum exhibits a characteristic peak at approximately 29.5 pC, corresponding to the Cherenkov light produced by electron-induced ionization and electromagnetic cascading in water.

The next steps involve simulating the response of the scintillator detector and of the RPCs to the secondary shower particles, so the hodoscope coincident trigger can be modeled.

It is expected that, when acquiring with the hodoscope trigger, only crossing muons will have a significant contribution, as virtually all electrons and decaying muons have their secondary particles fully stopped within the water volume.

## 5. Current status and prospects

The current setup of the CBPF hodoscope can be seen in Figure 6 and is mounted with a shallow "E tank", instrumented with the prototype multi-PMT developed by the team from the University of Naples [13], in order to characterize one of the proposed configurations for the SWGO outer array WCD unit.

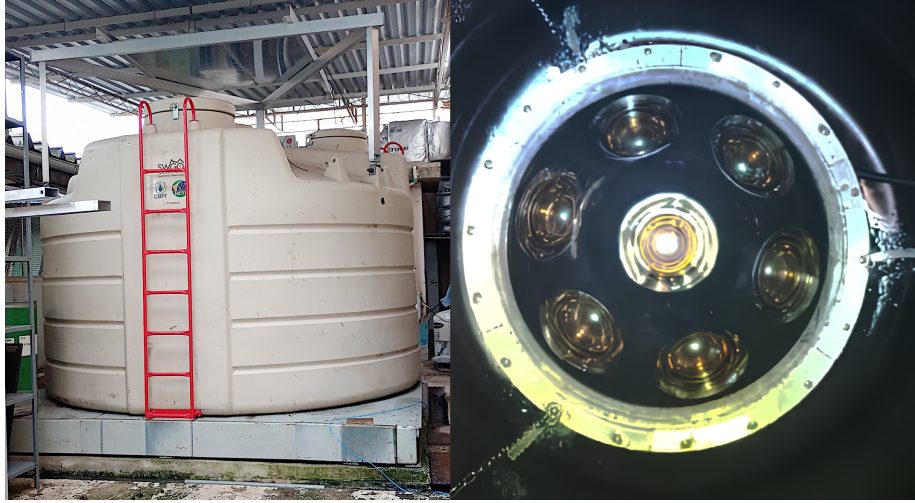


**Figure 6:** Left: Picture of the current hodoscope setup, with the shallow "E tank". Right: Picture of the multi-PMT module deployed inside the tank, as seen from above.

The first tests are being conducted to verify the angular distribution and heat maps of events (crossing muons) in the top and bottom hodoscope layers. The multi-PMT is collecting data to verify the light-tightness of the tank, as well as establishing baseline variations with temperature.

Once these preliminary tests are finished, the hodoscope will begin acquiring events in coincidence with the multi-PMT. The expected average rate of hodoscope triggers is between 40-60 Hz, considering the electronic efficiency after adjusting for high voltage in the RPCs and scintillator detectors due to day-time temperatures, and for ensuring a noise-free reading. It is expected that the set-up will thus acquire as much as 20 million events per week.

The setup will allow us to study in detail the response of the multi-PMT and other WCD unit configurations installed in the tank, using the muon tracks to calibrate the WCD response. This exercise is fundamental to benchmark and compare the different WCD configurations proposed for SWGO.

## References

- [1] Ruben Conceição. The southern wide-field gamma-ray observatory, 2023.
- [2] Pablo M. Bauleo and Julio Rodríguez Martino. The dawn of the particle astronomy era in ultra-high-energy cosmic rays. *Nature*, 458(7240):847–851, Apr 2009.
- [3] Ricardo Luz, P. Abreu, S. Andringa, P. Assisa, and Blanco et al. Marta’s (muon array with rpc for tagging air showers) daq system. page 098, 03 2020.
- [4] L.M. Domingues Mendes G. F. Franco B. S. González L.F. Mendes U. Barres de Almeida\*, P. Assis and others. The Mercedes water Cherenkov detector: a multi-PMT shallow tank design proposal for ground-based gamma-ray observatories. In *38th International Cosmic Ray Conference*, 2023.
- [5] OMEGA. MAROC3 Datasheet. Available online at <https://mega.nz/file/EFNk2RqK#yjl60Rtj400RJjkKIDFr-7YvmPkd-yuLtgZR99cabq0>.
- [6] Intel. Cyclone® IV FPGA Devices. Available online at <https://www.intel.com/content/www/us/en/products/details/fpga/cyclone/iv.html>.
- [7] TerasIC. DE-10 Standard. Available online at [url={https://www.terasic.com.tw/cgi-bin/page/archive.pl?CategoryNo=165&No=1081}](https://www.terasic.com.tw/cgi-bin/page/archive.pl?CategoryNo=165&No=1081), urldate = 2023-08-09, year = 2017.
- [8] Chris Hagmann, David Lange, and Douglas Wright. Cosmic-ray shower generator (cry) for monte carlo transport codes. In *2007 IEEE Nuclear Science Symposium Conference Record*, volume 2, pages 1143–1146, 2007.
- [9] Ilya G Usoskin, Sami K Solanki, Natalie A Krivova, Bernhard Hofer, Gennady A Kovaltsov, Lukas Wacker, Nicolas Brehm, and Bernd Kromer. Solar cyclic activity over the last millenium reconstructed from annual 14c data. *Astronomy & Astrophysics*, 649:A141, 2021.
- [10] Sea Agostinelli, John Allison, K al Amako, John Apostolakis, H Araujo, Pedro Arce, Makoto Asai, D Axen, Swagato Banerjee, GJNI Barrand, et al. Geant4—a simulation toolkit. *Nuclear instruments and methods in physics research section A: Accelerators, Spectrometers, Detectors and Associated Equipment*, 506(3):250–303, 2003.
- [11] Geant4 Collaboration. *Geant4 Physics Reference Manual*. Geneva, Switzerland, 2023. Available online at <https://geant4-userdoc.web.cern.ch/UsersGuides/PhysicsReferenceManual/>.
- [12] P. Allison et al. Observing muon decays in water Cherenkov detectors at the Pierre Auger Observatory. In *29th International Cosmic Ray Conference*, 8 2005.
- [13] Matteo Tambone. Photosensors and electronics characterization of the multipmt prototype for the swgo experiment. Master’s thesis, Università degli Studi di Napole "Federico II", 2024., 2024. Available online at [https://www.fisica.unina.it/documents/12375590/13725484/3463\\_TamboneM.pdf/b5dc521f-ebd8-491c-8afc-63b28f96f721](https://www.fisica.unina.it/documents/12375590/13725484/3463_TamboneM.pdf/b5dc521f-ebd8-491c-8afc-63b28f96f721).